

# Precise measurement of the dielectric properties of $\text{Ba}_x\text{Sr}_{1-x}\text{TiO}_3$ thin films by on-wafer through-reflect-line (TRL) calibration method

G. Bhakdisongkhram\*, S. Okamura, T. Shiosaki

Graduate School of Materials Science, Nara Institute of Science and Technology (NAIST),  
8916-5 Takayama-cho, Ikoma, Nara 630-0192, Japan

Available online 8 November 2005

## Abstract

Polycrystalline  $\text{Ba}_x\text{Sr}_{1-x}\text{TiO}_3$  ( $x=0.3, 0.4, 0.5$ ) (BST) thin films with a thickness of 200 nm were deposited on r-cut sapphire substrates by rf sputtering method. The permittivity and loss tangent of the films were successfully observed in the range of 1–3 GHz, by utilizing the on-wafer through-reflect-line (TRL) calibration method although the estimated relative permittivity depended on an applied power to waveguides and the loss tangent had the dispersion around 1 GHz even in the case of 2  $\mu\text{m}$ -thick aluminum. Finally, we concluded that the BST thin film with  $x=0.4$  is the most suitable for microwave tunable devices because it had the lowest loss tangent and relatively high permittivity.

© 2005 Elsevier Ltd. All rights reserved.

**Keywords:** BST; Films; Dielectric properties; Electrical properties; Perovskites

## 1. Introduction

Thru-Reflect-Line (TRL) calibration method has been widely used for more than 20 years because of its efficiency and accuracy. Meanwhile, the probing of the microwave integrated circuits goes to the wafer level, due to their tiny sizes. The combination of the TRL calibration method and the on-wafer test method make it possible to accurately determine both attenuation constant and phase of the propagating wave on the waveguide lines upon a multilayer substrate. For thin films, this technique allows the measurement of the dielectric loss and dielectric constants on a continuous frequency range, which is not possible with the resonator method. The present technique has been successfully used with the semiconductor substrates for a decade. However, the application of this technique to the high-k films such as  $\text{Ba}_x\text{Sr}_{1-x}\text{TiO}_3$  (BST) has been tested only recently.<sup>1,2</sup> This paper describes the precise measurement of the permittivity and loss tangent of the BST ( $x=0.3, 0.4, 0.5$ ) thin films by on-wafer Thru-Reflect-Line calibration method.

## 2. Experimental

Polycrystalline  $\text{Ba}_x\text{Sr}_{1-x}\text{TiO}_3$  ( $x=0.3, 0.4, 0.5$ ) thin films were deposited on 0.5 mm-thick r-cut sapphire substrates at

600 °C for 60 min by rf-magnetron sputtering. Substrates and BST powder targets were positioned parallel to each other with a distance of 3.5 cm. Sputtering gas pressures were set to be 1.3 Pa for  $x=0.3$ , 4.0 Pa for  $x=0.4$ , and 6.7 Pa for  $x=0.5$ . The gas pressure ratio of Ar to  $\text{O}_2$  was 9:1. The crystal structure of deposited films was confirmed by X-ray diffraction analysis (XRD) and the surface morphology was observed by scanning electron microscopy (SEM).

Coplanar “Thru” and “Line” test patterns were formed on the BST thin films by a conventional photolithography technique. Homogeneous aluminum thin films with a thickness of 0.5, 1.0 or 2.0  $\mu\text{m}$  were deposited on the BST/sapphire substrates by vacuum evaporation, and then they were patterned by wet-etching. The Shipley S1813 (Rohm and Hass Electronic Materials) was used as a photoresist and an etchant for aluminum was Semico Clean (Furuuchi Chemical Corporation). The widths of a signal line and a gap were designed to be 30 and 20  $\mu\text{m}$ , respectively as the characteristic impedance of waveguides will be 50  $\Omega$  when relative permittivity of BST thin films is 400. The “Line” patterns had meandering signal paths with a length of 1 cm.

Microwave measurement was carried out with the HP8753D network analyzer in the frequency range from 1 to 3 GHz with an applied power of 0 dBm. The propagation constant was extracted from S-parameters of the “Thru” and “Line” patterns by the following equation<sup>3</sup>:

\* Corresponding author.

$$e^{-\gamma l} = \frac{L_{21}^2 + T_{21}^2 - (T_{11} - L_{11})^2 \pm \sqrt{\{L_{21}^2 + T_{21}^2 - (T_{11} - L_{11})^2\}^2 - 4L_{21}^2 T_{21}^2}}{2L_{21}T_{21}} = \alpha e^{-j\beta l} \tag{1}$$

where  $\gamma$  is a propagation constant,  $\alpha$  an attenuation constant,  $\beta$  a phase constant,  $T_{11}$  and  $T_{21}$  are the reflection coefficient and the transmission coefficient of the “Thru” pattern,  $L_{11}$  and  $L_{21}$  are the reflection coefficient and the transmission coefficient of the “Line” pattern. The relative permittivity and loss tangent of the BST thin films were extracted from the propagation constant.

### 3. Results and discussion

#### 3.1. Preparation of coplanar waveguides

The thickness of deposited films for 60 min was approximately 200 nm, that is, the deposition rate was 3.3 nm/min. It is confirmed by XRD that all the deposited films were crystallized into perovskite BST with (1 1 1)-preferred orientation. They had smooth surface and dense structure as shown in Fig. 1. The resistivity of the aluminum films was estimated to be  $1.741 \times 10^{-4} \Omega \text{ cm}$  by the four-point-probe resistivity measurement. Fig. 2(a) and (b) shows the SEM images of the “Thru” and the “Line” patterns. The widths of the signal line and the gap (see Fig. 2(c)) were designed to be 30 and 20  $\mu\text{m}$ , respectively. However, practical widths of the signal line and the gap were varied with the aluminum thickness due to the difference of etching conditions. Therefore, the applied power to these waveguides was different due to impedance mismatching as shown in the Table 1.

#### 3.2. Estimation of permittivity

The propagation constants of  $\text{Ba}_x\text{Sr}_{1-x}\text{TiO}_3$  ( $x=0.3, 0.4, 0.5$ ) thin films were measured with waveguide thicknesses of 0.5, 1.0 and 2.0  $\mu\text{m}$ . The relationships between the phase constant  $\beta$  and the frequency derived from these results were shown in Fig. 3. The effective permittivities  $\epsilon_{\text{eff}}$  of the samples were estimated from the slopes of the phase-frequency relationship as follows:

$$\frac{\Delta\beta}{\Delta f} = \frac{2\pi}{c} \sqrt{\epsilon_{\text{eff}}} \tag{2}$$

where  $f$  is a frequency,  $c$  the light velocity in vacuum. The relative permittivity of the BST layer  $\epsilon_{\text{BST}}$  was extracted from the

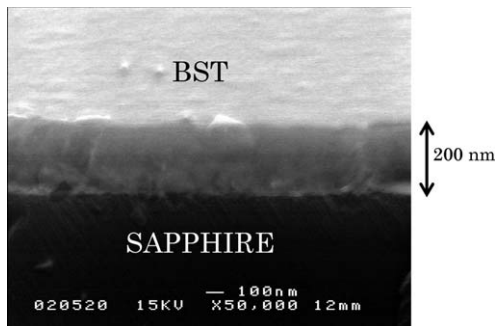
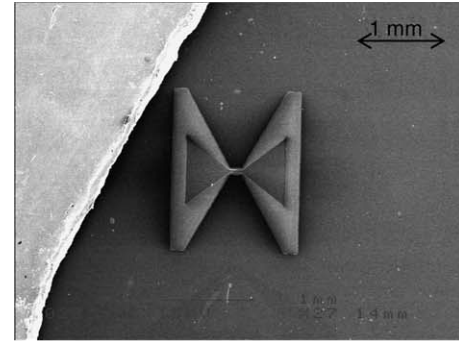
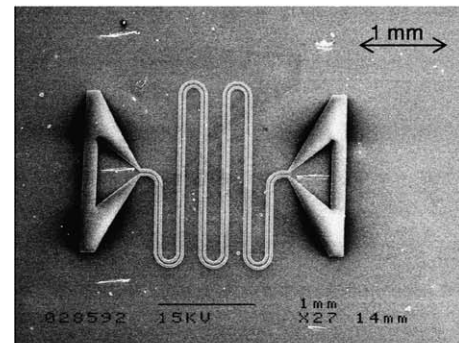


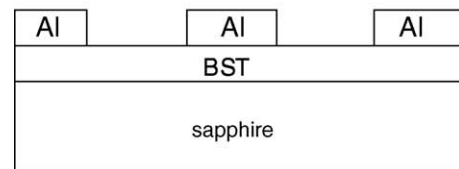
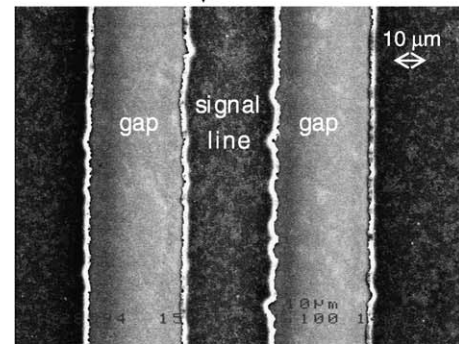
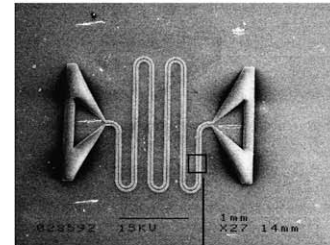
Fig. 1. SEM image of the sputtered BST film ( $x=0.5$ ) on a sapphire substrate.



(a)



(b)



(c)

Fig. 2. (a) SEM images of the “Thru” patterns; (b) SEM images of the “Line” patterns; (c) SEM image of the signal line and the gap after wet-etching.

Table 1  
Specification of fabricated coplanar waveguides

Case	Al thickness ( $\mu\text{m}$ )	Line width ( $\mu\text{m}$ )	Gap width ( $\mu\text{m}$ )	Measured characteristic impedance ( $\Omega$ )	Estimated applied power (dBm)
1	0.5	35	22	106	–28
2	1.0	30	27	68	–15
3	2.0	28	28	61	–10

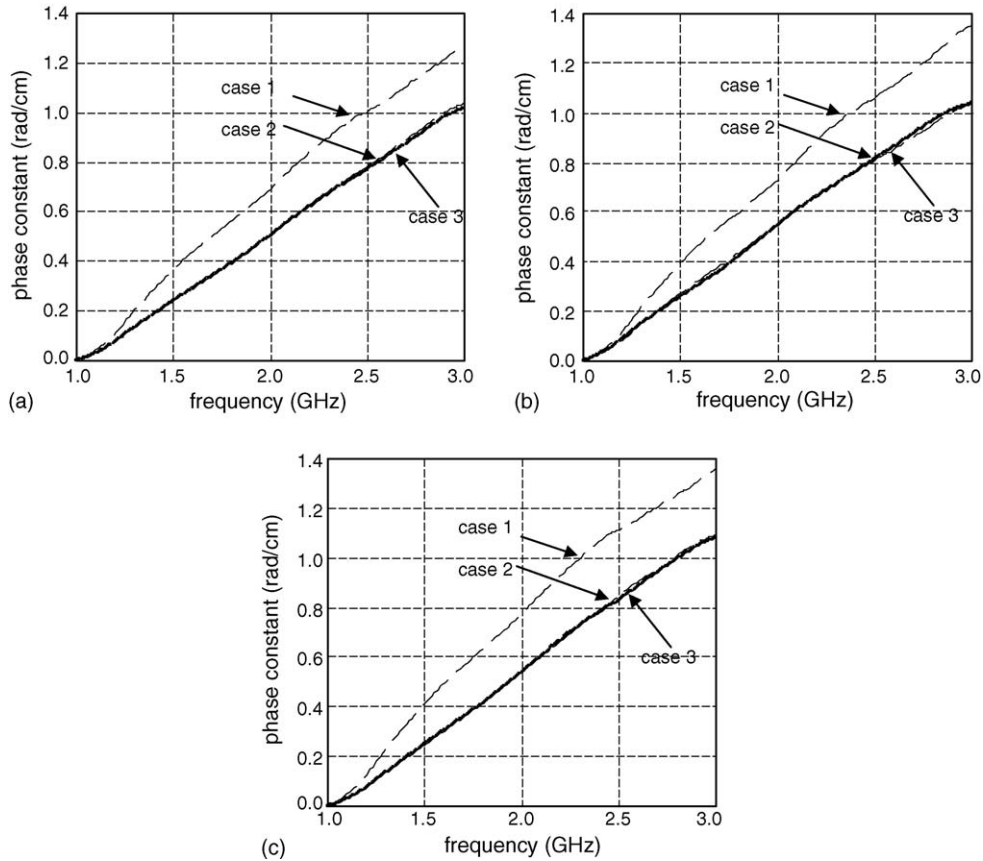


Fig. 3. Phase constant–frequency relation of the signal on the coplanar waveguide when (a)  $x=0.3$ , (b)  $x=0.4$ , (c)  $x=0.5$ .

effective permittivity  $\epsilon_{\text{eff}}$  by conformal mapping method as follows:

$$\epsilon_{\text{eff}} = 1 + 0.500 \times (\epsilon_{\text{sapphire}} - 1) + 0.003 \times (\epsilon_{\text{BST}} - \epsilon_{\text{sapphire}}) \quad (3)$$

for the case when the width of signal line and gap are 30 and 20  $\mu\text{m}$ , thickness of the BST layer and sapphire substrate are 200 nm and 500  $\mu\text{m}$ , and  $\epsilon_{\text{sapphire}}$  (=10) is the permittivity of the sapphire substrate.

The relative permittivities of the BST thin films are shown in Table 2 (the relative permittivity values for case 1 are not shown because the values are out of calculation range). It is found that the relative permittivity depends on the applied power. Higher applied power resulted in lower permittivity. It seems that the tunability of BST thin films corresponded to this applied power dependence of the permittivity.

### 3.3. Estimation of loss tangent

The effective loss tangent  $\tan \delta_{\text{eff}}$  was extracted from the attenuation constant and the effective permittivity as follows:

$$\alpha = 0.91 \sqrt{\epsilon_{\text{eff}}} f(\text{GHz}) \tan \delta_{\text{eff}} \quad (4)$$

Table 2  
Relative permittivity of  $\text{Ba}_x\text{Sr}_{1-x}\text{TiO}_3$  thin films with different applied power

Case	Estimated applied power (dBm)	Relative permittivity		
		$x=0.3$	$x=0.4$	$x=0.5$
1	–28	–	–	–
2	–15	358.7	421.0	681.6
3	–10	288.9	354.4	615.9

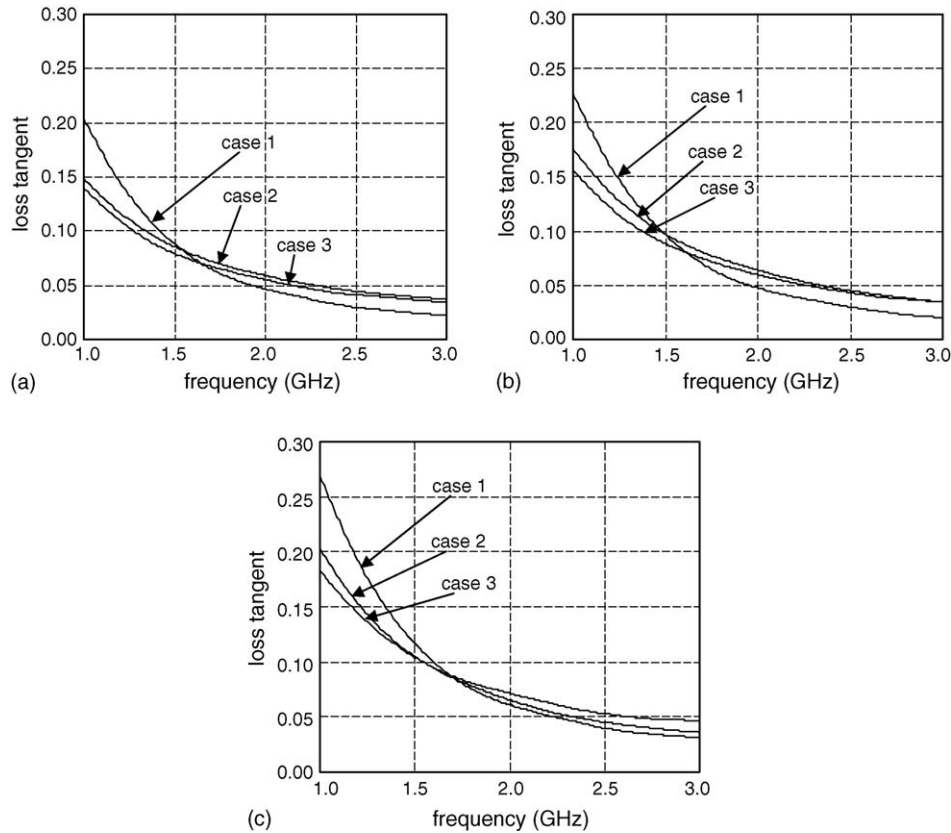


Fig. 4. Tangent loss of the BST layer when (a)  $x=0.3$ , (b)  $x=0.4$ , (c)  $x=0.5$ .

The loss tangent of the BST  $\tan \delta_{\text{BST}}$  was also extracted from the effective loss tangent by conformal mapping method as follows:

$$\tan \delta_{\text{BST}} = \frac{\varepsilon_{\text{eff}} \tan \delta_{\text{eff}}}{0.003 \times \varepsilon_{\text{BST}}} \quad (5)$$

for the same case to Eq. (3), and the loss tangent of the sapphire substrate was neglected because it was more than two orders lower than that in the BST layer.

Fig. 4 shows the loss tangents as the function of frequency. In any cases, the dispersion was observed around 1 GHz and the level of the dispersion depended on the thickness of aluminum layers. Thinner aluminum layers caused larger loss tangent. It seems that this is due to conductor thickness being much lower than the skin depth, so that the magnetic field can penetrate significantly through the conductor, under such a situation the assumed pure TEM mode no longer exists and thus causes a larger attenuation than expected. Moreover, for the BST single crystal, emission of an ultrasonic wave from the gap of a waveguide due to electrostriction can be possible around 1–2 GHz.<sup>4</sup> To understand the mechanism of such attenuation, further study is needed. It is found that the thickness 2  $\mu\text{m}$  of the aluminum layer was not enough for precise measurement of dielectric properties in the frequency range of 1–3 GHz, where the skin depth was around 2.5  $\mu\text{m}$ .

From the above investigation, we concluded that the 2  $\mu\text{m}$ -thick aluminum layer was better. Therefore, we compared the dielectric properties of BST thin films with  $x=0.3$ , 0.4 and 0.5

Table 3

Dielectric properties of  $\text{Ba}_x\text{Sr}_{1-x}\text{TiO}_3$  thin films estimated by the on-wafer TRL calibration method

$x$	Sputtering pressure (mTorr)	Relative permittivity (1–3 GHz) (@ power –10 dBm)	Loss tangent @ 3 GHz (@ power –10 dBm)
0.3	10	288.9	0.037
0.4	30	354.4	0.035
0.5	50	615.9	0.046

and 2  $\mu\text{m}$ -thick aluminum layers as shown in Table 3. From this table, it is found that the BST thin film with  $x=0.4$  had the low loss tangent and relatively high permittivity. It seems that the BST thin film with  $x=0.4$  is the most suitable for microwave tunable devices.

#### 4. Conclusions

Polycrystalline  $\text{Ba}_x\text{Sr}_{1-x}\text{TiO}_3$  ( $x=0.3, 0.4, 0.5$ ) thin films with a thickness of 200 nm were deposited on r-cut sapphire substrates by rf sputtering method and their microwave properties were evaluated by on-wafer TRL calibration method. The relative permittivity estimated by the on-wafer TRL calibration method depended on the applied power due to non-linearity of the permittivity of BST thin films. It is found that the thickness of conductors had a great influence on the loss tangent properties. Even 2  $\mu\text{m}$ -thick aluminum layer was not enough for precise measurement of dielectric properties in the frequency

range of 1–3 GHz. Furthermore, the dispersion of loss tangent was observed around 1 GHz. The investigation of this dispersion is the future work.

## References

1. Lue, H. T. and Tseng, T. Y., Application of on-wafer TRL calibration on the measurement of microwave properties of  $\text{Ba}_{0.5}\text{Sr}_{0.5}\text{TiO}_3$  thin films. *IEEE Trans. Ultrasonics Ferroelectr. Freq. Contr.*, 2001, **48**, 1640–1647.
2. Delprat, S., Ouaddari, M., Vidal, F., Chaker, M. and Wu, K., Voltage and frequency dependent dielectric properties of BST-0.5 thin films on alumina substrates. *IEEE Microwave Wireless Comp. Lett.*, 2003, **13**, 211–213.
3. Pozar, D. M., *Microwave Engineering (2nd ed.)*. John Wiley and Sons, New York, 1998, pp. 217–221.
4. Vendik, O. G. and Zubko, S. P., Modeling microwave dielectric characteristics of thin ferroelectric films for tunable planar structures. *Integrated Ferroelectr.*, 2001, **34**, 215–226.